ACTA GRAPHICA 234

# Performance Assessment of Three Rendering Engines in 3D Computer Graphics Software

## Authors

Žan Vidmar, Aleš Hladnik, Helena Gabrijelčič Tomc*

*University of Ljubljana*
*Faculty of Natural Sciences and Engineering*
*Slovenia*
*\*E-mail: helena.gabrijelcic@ntf.uni-lj.si*

## Abstract:

The aim of the research was the determination of testing conditions and visual and numerical evaluation of renderings made with three different rendering engines in Maya software, which is widely used for educational and computer art purposes. In the theoretical part the overview of light phenomena and their simulation in virtual space is presented. This is followed by a detailed presentation of the main rendering methods and the results and limitations of their applications to 3D objects. At the end of the theoretical part the importance of a proper testing scene and especially the role of Cornell box are explained. In the experimental part the terms and conditions as well as hardware and software used for the research are presented. This is followed by a description of the procedures, where we focused on the rendering quality and time, which enabled the comparison of settings of different render engines and determination of conditions for further rendering of testing scenes. The experimental part continued with rendering a variety of simple virtual scenes including Cornell box and virtual object with different materials and colours. Apart from visual evaluation, which was the starting point for comparison of renderings, a procedure for numerical estimation and colour deviations of renderings using the selected regions of interest in the final images is presented.

## Keywords:

3D Computer Graphic, Rendering Algorithm, Testing Conditions
Colour Difference, Visualisation

## 1. Introduction

The history of investigations in the field of 3D computer generated graphics shows that a great effort was invested in the development of rendering algorithms, simulation of light interactions with different materials, visual perception of 3D sufrace phenomena and computer graphics (CG) colour reproduction and visualisations in various applications (Goesele, 2004; Paviotti, 2007; Ruppertsberg, 2007; Xiao, 2008; Menk, 2013; Fleming, 2003). An evidence for this are numerous scientific publications and integration of these algorithms in rendering engines, which enable different solutions and levels of photorealism of rendering outputs (Kajija, 1980; Jensen, 1996; Lafortune, 1993; Pharr, 2010; Murat, 2009). Countless web forums present experiments of individual enthusiasts and endless discussions about which engine is capable of better results for a specific computer generated scene or situation. On the other hand, references lack more rigorous approaches, test scenes and criteria for analysis that could help a user to more objectively compare and evaluate final renderings and choose the most suitable rendering engine. The aim of the study was to define the procedure for evaluation of renderings made with three different rendering engines in Maya software (Autodesk). The problem was analysed from many aspects: usability of engines, rendering settings, visual evaluation and colourimetrical evaluation (Hunt, 2011).

## 2. Theoretical part

From the beginnings of CG, scientists and engineers have striven to improve results in the light phenomena simulation. The basic goal was to consider physical, optical and energetic properties of light, which should be somehow interpreted in the 3D virtual world (Appel, 1968; Bouknigh, 1970; Phong, 1975; Blinn, 1976; Whitted, 1980). The main task, which is an active field of research also nowadays, is to develop a method and combination of algorithms that would be able to render photorealistic reproduction in an acceptable rendering time. Within a simplified scheme the incident light can be divided into reflected, absorbed, scattered and transmitted light, the proportions of which are defined by the properties and appearance of material. The simulations of these light phenomena, which are included in rendering equations, also enable the reproduction of computer generated light (Birn, 2013; Erzetič, 2010; Kočevar, 2013). Render engine is a piece of programming code, which enables the final image output or sequence of images (renderings) of 3D computer generated world. In technical terms rendering includes calculations performed by a render engine, which translates the scene from a mathematical approximation to a 2D image. The techniques that are the most widely used and popular in rendering engines are: ray tracing, path tracing, photon mapping, bidirectional path tracing and unbiased rendering. Apart from these, light tracing, distributed ray tracing, metropolis light transport, stochastic progressive photon mapping (SPPM), beam tracing, cone tracing have also been used frequently (Pharr, 2010).

In *ray tracing*, rays start their paths in camera. The visualisation of virtual scene is generated in image area, where the ray's path is calculated for each pixel. So called primary rays or view rays encounter the virtual objects and are reflected (reflective rays) or refracted (refractive rays). When a ray hits the object in the area, from which it cannot be reflected directly to the light source, a shadow is formed (shadow ray) (Appel, 1968; Whitted 1980). In *path tracing*, each ray is in its path traced from the camera to the light source. When the light source is found, the total contribution of light reflected by different materials and other potential virtual contributors are calculated on the path. In addition to the lights, the background is considered as a light source as well. Path tracing is suitable for illumination of exteriors and scenes with easily accessible light sources (Yafaray, 2009; Krishnamachari, 2004; Csébfalvi, 1997; Kajiya, 1986).

*Photon mapping* was developed by the Danish researcher Henrik Wann Jensen, which in his thesis presented a process that in the first step generates photon map and in the second

one renders it with the use of ray tracing (Jensen, 2001; Jensen, 2002). As the result of the first step, i.e. photon map, is a grainy visualisation, additional algorithms for corrections such as final gathering are usually needed. In comparison to ray tracing, photon mapping simulations of real world phenomena are more accurate. This technique treats light as a group of particles (photons), whose calculation starting point is in the light source. Moreover, photon mapping takes into account final gathering, indirect lighting, caustics and dispersion (Yafaray, 2009; Luxrender, 2013; Pharr, 2010; Krishnamachari, 2004).

*Bidirectional path tracing* is based on BRDF (Bidirectional Reflectance Distribution Function) and is in practical terms a combination of positive properties of photon mapping and path tracing. Bidirectional path tracing is a method with simultaneous tracking of rays coming from the light source (light path), which travel via camera, and from camera (eye path, camera path), which travel via light source. After tracking the paths of a high number of rays from both sides, the rays are connected and image pixels are generated. Taking into account long rendering time, quality of renderings is very high and the visualisations are physically accurate (Lafortune, 1993; Adamsen, 2009; Pajot, 2011; Bogolepov, 2013).

Unbiased rendering - This physically based rendering procedure is defined as a rendering technique that does not introduce any systematic error into the radiance approximation and as a result theoretically enables a perfect photorealism. Due to a combination of many algorithms it contains, such as path tracing, light tracing, bidirectional path tracing, metropolis light transport and stochastic progressive photon mapping and since it considers all light interaction phenomena (global illumination, indirect lighting, caustics, ambient occlusion, etc.) the Unbiased final rendering is often taken as a reference point for other rendering techniques. Apart from some adjustments of camera and the number of samples influencing the noise of an image and photorealistic effects, the user has almost no control on the quality of renderings. In spite of, in physical terms, an apparently perfect rendering technique, some serious restrictions limit its use. (Pharr, 2010; Kouhzadi, 2013; Maxwell, 2014).

Cornell box was introduced in 1984 at the Cornell University, with a purpose of testing the interaction between diffuse surfaces and light and comparing computer generated renderings with photographic images (Goral, 1984). Referential image was usually a photograph of real physical objects or settings, while the test image was computer generated. In spite of some minor changes (original box had red and blue walls and no light source), Cornell box is still a very popular test model with one light source in the middle of the white ceiling, green wall on the right, red wall on the left and white back wall and floor. In the scene, 3D objects are positioned in the middle of the box.

## 3. Experimental part

In the experimental part three rendering engines in Autodesk Maya 2014´64 (software for 3D computer animation, modelling, simulation, rendering and compositing) were analysed. The specifications of hardware and software (Maxwell, 2014; O'Connor, 2010; Sannino, 2013) used in the research are presented in Table 1.

The study consisted of five steps. The first step was the scene setting, i.e. modelling, texturing and lighting of Cornell Box, which provided the same conditions for all three engines. The second and the third step were the definition of the rendering quality for further testing and correction of differences between the outputs of individual rendering engines. The fourth and fifth steps were rendering of scenes and visual and colourimetrical analysis of rendering results. The dimensions of Cornell box were: length = 800 units, width = 300 units, height = 300 units. The centre of the box was positioned in the coordinate centre, xyz = (0, 0, 0). Virtual lighting included area light with the side length of 100 units and position xyz = (0, 149.999, -200). Two

cameras with 25 mm lenses were used. First camera with rotation coordinates xyz = (0, 0, 0) was positioned in xyz = (0, 0, 399.999), while the second camera had position in xyz = (0, 145, 100) and rotation coordinates xyz = (-45, 0, 0). The materials of Cornell box were completely diffuse without reflection. Left wall of the box was red (HSV= 0, 179, 179), right wall was green (HSV = 120, 179, 179), while the other walls, the ceiling and the floor were gray (HSV = 0, 0, 179). Colour values of testing object (sphere) were HSV= 0, 0, 179.

## 3.1 DETERMINATION OF PARAMETERS FOR RENDERING ENGINES COMPARISON

An objective and unbiased comparison of modern rendering engines and their output images is anything but a simple task. When there is no limitation in rendering time and number and combination of settings, the results for all engines, which include advanced illumination and rendering algorithms, can be very similar and more or less photorealistic. Consequently, at least one constraint has to be used for an

*Table 1. Hardware and software specifications.*

| | Hardware | | Rendering engines |
|---|---|---|---|
| CPU | Intel Xeon CPU E31275, 3.40GHz (Quad-core – 4 simulated) | 1 | Next Limit Technologies Maxwell Render Version 2.7.10.0. x64 |
| HD | Intel SSD 240GB, 335 series | 2 | mental ray for Maya 2014 Version 3.11.1.4, (2013), revision 189569 |
| RAM | 32GB (ECC) | | Chaos Group V-Ray V-Ray for Maya version 2.30.01,V-Ray core version is 2.00.01 |
| GPU | Nvidia Quadro 4000 (2GB GDDR5) | 3 | |
| OS | Microsoft Windows 7 Ultimate (64) | | |

*Table 2. Rendering time in dependence of the sampling quality (a.) and rendering time in dependence of indirect illumination settings (b.), where R = Ray trace, GI = Global Illumination, C = Caustic, FG0 = Final Gathering + 0 second bounces, FG5 = Final Gathering + 5 second bounces and IP = Irradiance Particles (mental ray).*

| a.) | | b.) | | | |
|---|---|---|---|---|---|
| Samp. quality | Rend. time (hh:mm:ss) | No. | Combination of functions | Rendering time | Result |
| 0.01 | 0:01:02 | 1 | R | 0:01:35 | |
| 0.50 | 0:01:05 | 2 | R + GI | 0:01:10 | |
| 1.00 | 0:01:08 | 3 | R + C | 0:01:31 | |
| 1.50 | 0:01:09 | 4 | R + FG0 | 0:01:34 | |
| 2.00 | 0:01:17 | 5 | R + FG5 | 0:01:47 | |
| 2.50 | 0:01:20 | 6 | R + I | 0:05:27 | |
| 3.00 | 0:01:24 | 7 | R + GI + C | 0:01:26 | |
| | | 8 | R + GI + FG0 | 0:01:34 | |
| | | 9 | R + GI + FG5 | 0:01:40 | |
| | | 10 | R + GI + IP | 0:05:20 | |
| | | 11 | R + C + FG0 | 0:01:56 | |
| | | 12 | R + C + FG5 | 0:01:54 | good rendering quality |
| | | 13 | R + C + IP | 0:05:26 | |
| | | 14 | R + FG0 + IP | 0:02:58 | |
| | | 15 | R + FG5 + IP | 0:04:43 | |
| | | 16 | R + GI + C + FG0 | 0:01:43 | excellent rendering quality and shortest rendering time |
| | | 17 | R + GI + C + FG5 | 0:01:44 | excellent rendering quality |
| | | 18 | R + GI + C + IP | 0:05:29 | |
| | | 19 | R + GI + FG0 + IP | 0:02:53 | |
| | | 20 | R + GI + FG5 + IP | 0:04:51 | |
| | | 21 | R + C + FG0 + IP | 0:03:01 | |
| | | 22 | R + C + FG5 + IP | 0:04:52 | good rendering quality |
| | | 23 | R + GI + C + FG0 + IP | 0:02:57 | |
| | | 24 | R + GI + C + FG5 + IP | 0:04:59 | good rendering quality |

*Table 3. Rendering time in dependence of the number of samples (Maxwell Render).*

| No. of samples | Rend. time (hh:mm:ss) | No. of samples | Rend. time (hh:mm:ss) | No. of samples | Rend. time (hh:mm:ss) |
|---|---|---|---|---|---|
| 1 | 0:00:10 | 10 | 0:05:07 | 18 | 2:15:51 |
| 2 | 0:00:13 | 11 | 0:07:25 | 19 | 3:16:24 |
| 3 | 0:00:17 | 12 | 0:10:47 | 20 | 4:17:09 |
| 4 | 0:00:24 | 13 | 0:15:30 | 21 | 6:24:32 |
| 5 | 0:00:44 | 14 | 0:23:23 | 22 | 9:35:17 |
| 6 | 0:01:18 | 15 | 0:34:37 | 23 | 14:22:40 |
| 7 | 0:01:42 | 16 | 0:51:35 | 24 | 21:31:16 |
| 8 | 0:02:28 | 17 | 1:29:40 | 25 | 32:07:38 |
| 9 | 0:03:33 | | | | |

objective evaluation. In our case the rendering criteria were: 1. quality, which was defined on the basis of visual evaluation of final renderings in terms of natural and photorealistic visualisation of light phenomena and light disposition and 2. rendering time, which was subordinate to quality. Therefore, in our testing procedure the criterion of the best rendering quality that can be obtained in maximum 60 minutes of rendering was used. On the basis of these criteria, internal standards and optimal settings were applied within each rendering engine.

*Mental ray* renderer has two main rendering settings, i.e. Quality and Indirect Lighting, each of them influencing the rendering time and visual quality. The sampling quality varied between 0.01 and 3 (Table 2). The results show that the quality value of 2 was optimal for our research, since it enabled the shortest rendering time with no observed visual noise artifacts in renderings. Next, the indirect illumination settings for mental ray were investigated. Apart from the default Ray trace setting, the settings also included six advanced functions: Global Illumination, Caustic, Importons (included in the setting of Irradiance Particles), Final Gathering, Irradiance Particles and Ambient Occlusion. As presented in Table 2, in our experiment several of these functions and their combinations were examined except for the Ambient Occlusion, which was not relevant for our 3D scenes. On the basis of visual evaluation of total 24 renderings, the following combination of functions producing excellent rendering quality and the shortest rendering time was chosen: Ray trace + Global Illumination + Caustic + Final Gathering + 0 second bounces (Figure 1).

*Maxwell render* has an extremely simple user interface. The only parameter that can be changed by the user is the number of samples, from minimum value of 1 to maximum of 30. The higher the number of samples, the longer the rendering time (affecting also image noise, as shown in Figure 1). In our first experiment, the number of samples was 25 and rendering time was 32 hours, 7 minutes and 38 seconds, which by far exceeded the predefined criteria of one hour. Subsequently, we experimented with a progressively higher number of samples – 1 to 25 (Table 3). Our experiments showed that when the number of samples exceeded 16, there was only an insignificant visual and noise difference found in the rendered images, but a great increase in rendering time was observed. Consequently, the number of samples equal to 16 was chosen as an optimal setting for Maxwell renderer.

The third investigated rendering engine was *V-Ray* with two main settings: threshold, which defines sampling threshold and the combination of engine parameters, which define the generation of primary and secondary bounces included in the global illumination. First testing step was again the determination of referential rendering conditions, i.e. its sampling threshold value (noise). Values ranging from 0.000 to 0.010, with a step of 0.001, were examined. Other rendering settings were left at their default values: global illumination, primary bounces engine: irradiance map, secondary bounces engine: Brute force and with active setting for Reflective Caustic and Refractive Caustic. Optimum value of sampling threshold of 0.003 and

rendering time 4 min 16 sec were chosen. Rendering time in dependence of the combination of primary and secondary bounces engines was measured and 16 renderings in total were visually analyzed (Table 4). As a result, optimum combination of Irradiance map (as primary bounces engine) and Light cache (as secondary bounces engine) with rendering time of 2 minutes and 15 seconds was selected (Figure 1).

The comparison of the number of settings and their combinations for three rendering engines are presented in Table 5.

### 3.2 CORRECTION OF LIGHT DISTRIBUTION IN RENDERED IMAGES

After setting the rendering parameters for the three investigated engines, colour deviations between the output images were evident, as can be seen in Figure 2. As each rendering engine has its own illumination system, the only possibility of correction was to correct brightness and contrast separately within the light settings of each engine in Maya software. The correction was performed by visually examining the three renderings and focusing on light disposition in the scene, which

*Table 4. Rendering time in dependence of the sampling threshold (a.) and of primary and secondary bounces (b.) in V-Ray.*

| a.) | | b.) | | | |
|---|---|---|---|---|---|
| Sampling threshold | Rendering time | No. | Primary bounces engine | Secondary bounces Engine | Rendering time (hh:min:sec) |
| 0.010 | 0:03:11 | 1 | Irradiance map | - | 0:03:00 |
| 0.009 | 0:03:13 | 2 | Photon map | - | 0:01:02 |
| 0.008 | 0:03:17 | 3 | Brute force | - | 0:07:21 |
| 0.007 | 0:03:20 | 4 | Light cache | - | 0:00:16 |
| 0.006 | 0:03:29 | 5 | Irradiance map | Photon map | 0:05:36 |
| 0.005 | 0:03:36 | 6 | Irradiance map | Brute force | 0:04:11 |
| 0.004 | 0:03:52 | 7 | Irradiance map | Light cache | 0:02:15 |
| 0.003 | 0:04:16 | 8 | Photon map | Photon map | 0:01:03 |
| 0.002 | 0:05:12 | 9 | Photon map | Brute force | 0:01:02 |
| 0.001 | 0:07:04 | 10 | Photon map | Light cache | 0:01:05 |
| 0.000 | 0:32:58 | 11 | Brute force | Photon map | 0:14:33 |
| | | 12 | Brute force | Brute force | 0:15:32 |
| | | 13 | Brute force | Light cache | 0:04:31 |
| | | 14 | Light cache | Photon map | 0:00:19 |
| | | 15 | Light cache | Brute force | 0:00:16 |
| | | 16 | Light cache | Light cache | 0:00:16 |

*Table 5. Number of settings and their combinations for mental ray – MR, Maxwell renderer – MX and V-Ray –VR.*

| Render engine | | Main settings | | Secondary settings | No. of comb. |
|---|---|---|---|---|---|
| MR | 2 | 1. quality 2. indirect lighting | 6 | 1. Global Illumination, 2. Caustic, 3. Importons (included in setting of Irradiance Particles), 4. Final Gathering, 5. Irradiance Particles 6. Ambient Occlusion | 24* |
| MX | 1 | no. of samples | - | - | 1 |
| VR | 2 | 1. threshold 2. combination of engines | 4 | 1. Irradiance map 2. Photon map 3. Brute force 4. Light cache | 16** |

*(see Table 2)

**(see Table 4)

was corrected for each of the three engines. Gamma value was set to 2.2 and bit depth to 8. The same corrected illumination conditions were applied also to other testing scenes using different materials, as discussed below.

## 4. Results

In the first step, Cornell box renderings were visually analysed. Output image of Maxwell renderer was the brightest, mental ray rendering had darker shadows and more evident bleeding (influence of reflectance of red and green wall on the colour of surrounding surfaces). V-Ray rendering had lower contrast, while light distribution was similar to that of Maxwell rendering. Inspite of the fact that the corrections of light disposition in the scenes were carried out carefully, some deviations still occurred due to the differences in rendering methods of the three engines. These deviations were also numerically analysed on altogether 19 regions of interests (ROIs) on our renderings (Figure 3). The default sRGB colour space was used in Maya (Autodesk), tiff file

format (lossless) and no conversions were used when RGB values of ROIs were determined with five measurements in image analysis software ImageJ (ImageJ 2014, Russ 2011). RGB values were converted into L*a*b* values of CIELAB colour space and mean and standard deviation values for each region were calculated. Mean and standard deviation values for $\Delta L^*$, $\Delta C^*_{ab}$ and $\Delta E^*_{ab}$ calculated for 19 renderings' ROIs of three engines: mental ray (MR), Maxwell (MX) and V-Ray (VR) are presented in Figure 3 and Table 6.

Figure 3 shows colour deviations between mental ray, Maxwell and V-Ray renderings after correction of light distribution. In general, the lowest differences are found between Maxwell and V-Ray, which differ especially in the brightest regions. This was not the case with the deviations between mental ray and Maxwell rendering, which colourimetrically differ mostly in the ROIs 1, 4, 5, 9, 10, and 19, and with the deviations between mental Ray and V-Ray, which were colourimetrically different especially in different regions of gray walls, i.e. ROIs 7, 8, 9, 10, 11, 18, and 19. In the subsequent research each rendering was analysed separately.
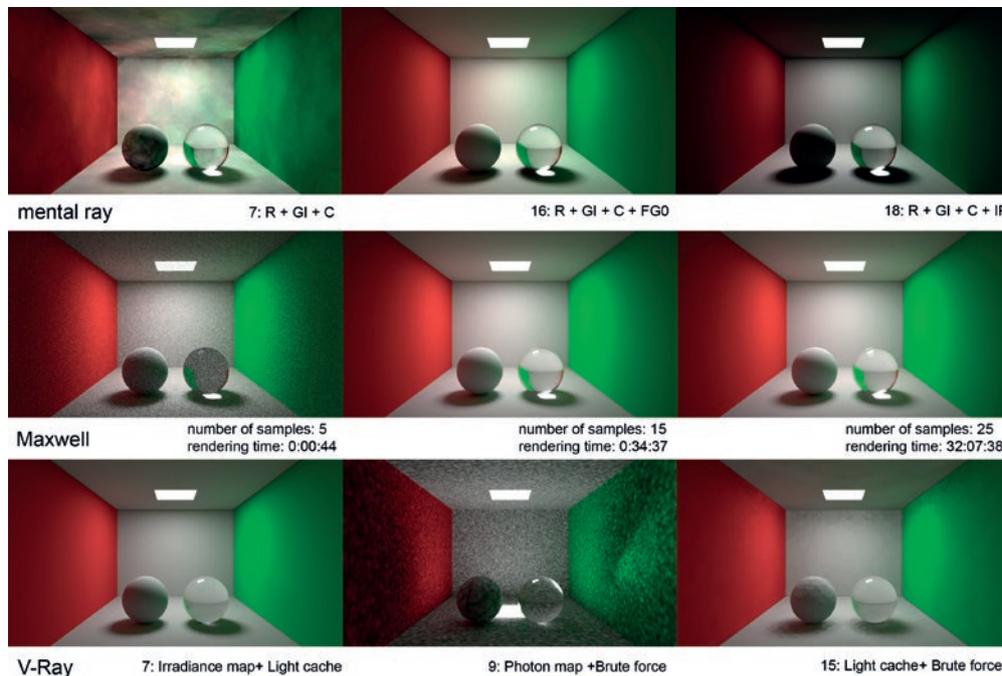


*Figure 1. Amount of noise in an image in dependence of the number of samples and rendering time (Maxwell render); quality of rendered images in dependence of the combination of functions (mental ray); examples of rendered image quality in dependence of the primary and secondary bounces (V-Ray).*

In Figure 4 presentations of colours for various ROIs in a*b* plain and on L* axis are shown. The highest chrominance (hue and chroma) ranges were found for Maxwell renderings, while this parameter is the lowest in the case of V-Ray engine. A larger difference between the brightest and the darkest point ($\Delta L^*$) was found in the case of mental ray, while V-Ray rendering has the lowest brightness range.

Next, differences in lightness ($\Delta L^*$), chroma ($\Delta C^*_{ab}$) and colour ($\Delta E^*_{ab}$) between representative ROIs were calculated (Figure 5). Colour differences were measured between ROIs: 1 and 2 (two regions of the red wall), 4 and 5 (two regions of the green wall), 7 and 16 (centre and the top left corner of the back wall), 9 and 10 (floor and sphere's umbra), 9 and 19 (floor and right bottom region of the back wall), 11 and 12 (the

brightest and right region of the sphere), 11 and 13 (the brightest and the centre of the sphere), 11 and 15 (the brightest and the darkest regions of the sphere), 12 and 15 (right and the darkest region of the sphere) and 13 and 15 (centre and the darkest region of the sphere).

In mental ray renderings there are in general the highest differences in brightness (consequently also values $\Delta E^*_{ab}$) between the selected regions of gray walls (Figure 5), while on Maxwell renderings ROIs on red and green walls (1 and 2, 4 and 5) and on the points of the sphere (12 and 15, 13 and 15) were reproduced with the highest colour deviations. Colour differences (consequently also differences in brightness and chroma) are in general the lowest in the case of the V-Ray rendering engine.
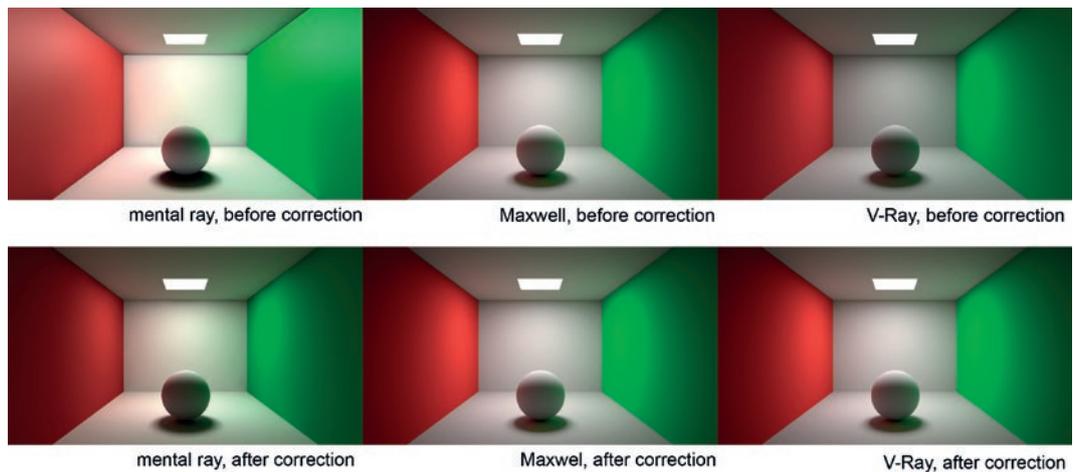


*Figure 2. Rendered images before and after correction of brightness, contrast, bit depth and gamma value: 1. mental ray, 2. Maxwell renderer, 3. V-Ray.*
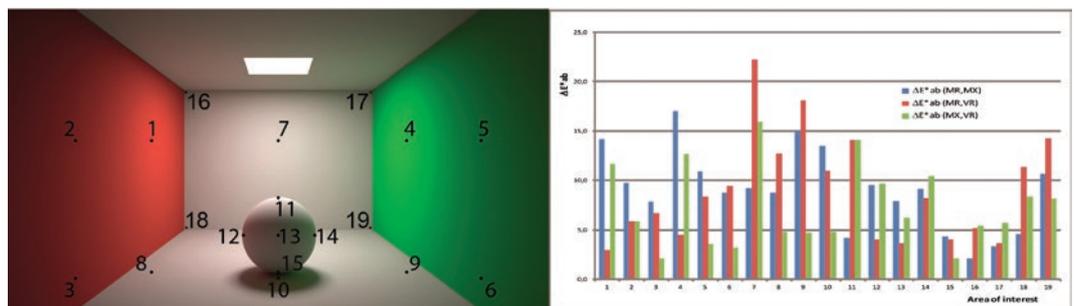


*Figure 3. 19 regions of interest and mean and standard deviation values for $\Delta L^*$, $\Delta C^*_{ab}$ and $\Delta E^*_{ab}$ calculated for 19 regions of interest.*

## 4.1 RENDERING OF SIMPLE SCENES WITH VARIOUS MATERIALS

The experimental part continued with the analysis of simple spheres-containing scenes including three different single sphere's materials: glass, mirror, plastic (scenes 2 to 4) and multiple colour spheres with diffuse, glass, mirror and plastic material (scenes 5 to 8). Spheres in the last three scenes (9 to 11) were characterized by variation in refraction index ranging from 0 to 2.0 (scene 9), reflectance from 0% to 100% with the step of 10% (scene 10) and transparency gradient from 0% to 100% with the 10% step (scene 11). In these experiments rendering time was measured and renderings (spheres and their surrounding environment) were visually analysed, taking into account: reflectance, bleeding, caustics, transmission and refraction. Scenes, material properties and rendering times are presented in Table 7.

Rendering time was, as expected, the longest in the case of Maxwell Render (mean value: 41 minutes and 51 seconds), while rendering times for the other two engines were 4 min and 20 seconds (mental ray) and 6 minutes 30 seconds (V-Ray), respectively. Visualisations of scenes 3, 5 and 9 are presented in Figure 6.

The *scene 3* – rendering of a mirror material (100% reflectivity) – visually appeared the same with all three rendering engines as shown in Figure 6. *Scene 5* with eleven colour spheres was set up with the purpose of analysing the distribution of indirect reflections, i.e. studying the influence of material, colour and optical properties on the surroundings. Spheres' colour varied in its hue value H, while S and V values were kept constant, i.e. HSV = (X, 179, 179). In comparison with Maxwell renderer, mental and V-Ray produced more pronounced simulation of indirect bounces (which is evident mostly on the two

*Table 6. Explanation of regions of interest (a.) and mean values of colour differences DE\*ab calculated for 19 regions of interest (b.)*

| a.) | | b.) | | |
|---|---|---|---|---|
| Point's No. (ROI) | Area of interest | difference | mean | stdv. |
| 1, 2, 3 | red wall | $\Delta L^*(MR,MX)$ | 5.4 | 3.3 |
| 4, 5, 6 | green wall | $\Delta L^*(MR,VR)$ | 6.6 | 5.3 |
| 7, 8, 9 | white wall | $\Delta L^* (MX,VR)$ | 5.7 | 4.5 |
| 10 | sphere's umbra | $\Delta C^*_{ab} (MR,MX)$ | 6.4 | 4.0 |
| 11 | brightest point of the sphere | $\Delta C^*_{ab} (MR,VR)$ | 5.1 | 3.1 |
| 12, 13, 14 | side parts of the sphere from red to green wall | $\Delta C^*_{ab} (MX,VR)$ | 2.9 | 2.8 |
| 15 | darkest point of the sphere (scene) | $\Delta E^*_{ab} (MR,MX)$ | 9.0 | 4.1 |
| 16, 17, 18, 19 | the corners of the back white wall | $\Delta E^*_{ab} (MR,VR)$ | 8.9 | 5.4 |
| | | $\Delta E^*_{ab} (MX,VR)$ | 7.3 | 4.1 |
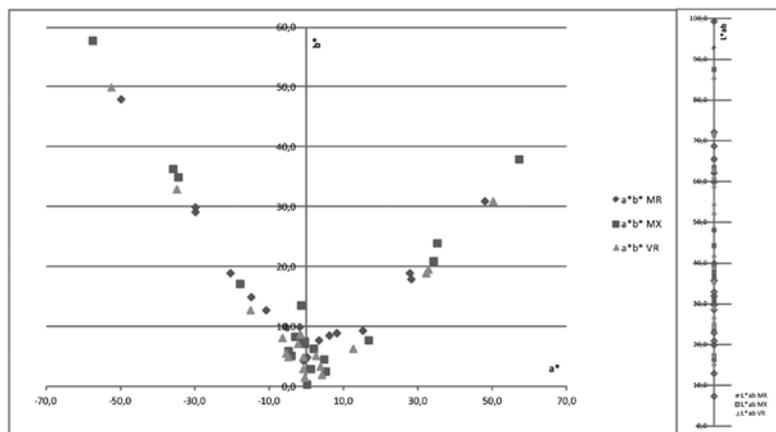


*Figure 4. Presentation of chrominance for different regions of interest in a\*b\* plane and presentation of brightness on L\* axis.*

bright spheres, orange and yellow) and less saturated colours of spheres (which can be explained as a result of an intense indirect lighting from the Cornell box walls). In *scene 9* spheres with various refraction indices ranging from 0 to 2.0 were rendered. In Figure 6 interesting rendering and visualisation phenomena can be observed. At this point it has to be stressed out that only V-Ray renderer permitted the refraction index with zero value, therefore the minimum values of 0.1 (mental ray) and 0.01 (Maxwell) were chosen for the other two rendering engines. As it could be expected from previously analysed scenes, visualisations and shadows are the darkest in the case of mental ray renderer, while different reproduction of refraction and a missing refraction of objects in the spheres can be seen in V-Ray rendering. Especially in the case of the refraction index of 1.0 (vacuum), there was a big difference in the reproduction from the three rendering engines, among which only the solution of Maxwell renderer matches the reality.
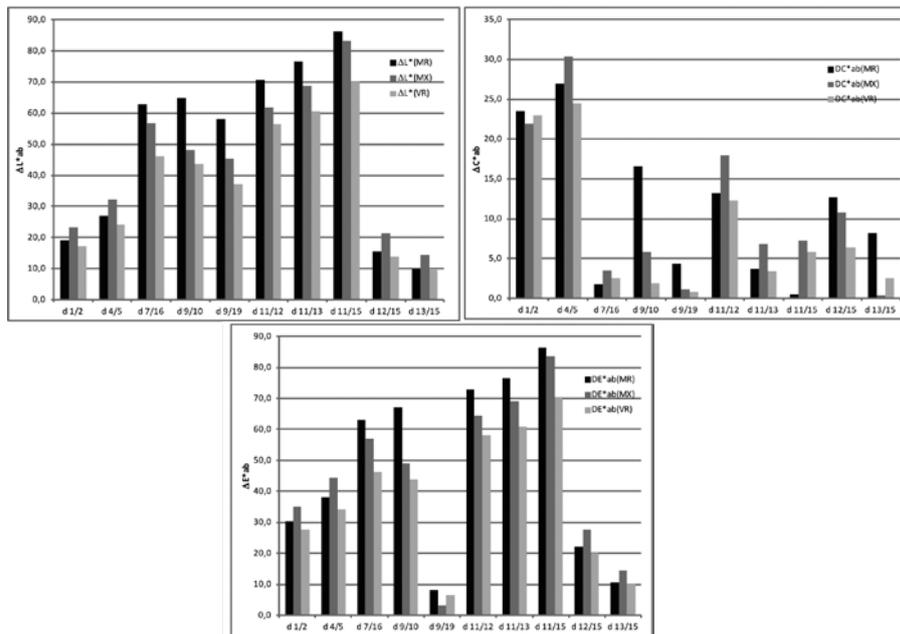


Figure 5. Values $\Delta L^*$, $\Delta C^*_{ab}$ and $\Delta E^*_{ab}$ calculated between different regions of interest on mental ray (MR), Maxwell (MX) and V-Ray (VR) renderings

Table 7. Cameras, materials and rendering time for eleven scenes rendered with mental ray, Maxwell and V-Ray.

| Scene | | | Rendering time (hh:min:sec) | | |
|---|---|---|---|---|---|
| No. | Camera | Material | mental ray | Maxwell | V-Ray |
| 1 | camera 1 | diffuse material | 0:01:43 | 0:29:44 | 0:01:49 |
| 2 | camera 1 | glass | 0:01:33 | 0:34:57 | 0:02:07 |
| 3 | camera 1 | mirror | 0:01:34 | 0:34:06 | 0:02:05 |
| 4 | camera 1 | plastic | 0:01:30 | 0:34:33 | 0:02:01 |
| 5 | camera 2 | colour diffuse material | 0:02:23 | 0:36:48 | 0:04:51 |
| 6 | camera 2 | colour glass | 0:05:47 | 0:55:15 | 0:12:02 |
| 7 | camera 2 | colour mirror | 0:06:09 | 0:39:08 | 0:08:15 |
| 8 | camera 2 | colour plastic | 0:03:28 | 0:43:32 | 0:08:16 |
| 9 | camera 2 | test of refraction index | 0:07:26 | 0:52:35 | 0:12:08 |
| 10 | camera 2 | gradient: diffuse to reflective materials | 0:06:40 | 0:48:38 | 0:07:45 |
| 11 | camera 2 | gradient of transparency | 0:05:55 | 0:51:05 | 0:10:12 |
| | Mean value: | | 0:04:20 | 0:41:51 | 0:06:30 |

*\*\*scenes from 5 to 11 with multiple spheres were rendered using camera 2, which enabled optimal field of view for the eleven analysed spherical objects.*

## 5. Conclusions

There is a lack of in-depth studies focusing on an objective determination of 3D software rendering quality. This is probably due to the vast range of available rendering methods, algorithms and principles, combinations of settings and software solutions. However, the issues of visualisation realism and reproduction accuracy of the interaction between the light and the surfaces (objects, materials) generated by various rendering engines are of prime importance to the 3D artists who are working in the field. In the research three rendering engines in Maya software were analysed in detail and compared to one another. The main findings are summarized below.

The number of rendering settings and their combinations was the lowest in the case of Maxwell renderer, where there is only one parameter that a user can adjust in comparison to 2 main parameters and 6 secondary settings in mental ray and 2 main parameters and 4 secondary settings in V-Ray. Consequently, the number of tested combinations differs from 1 for Maxwell renderer, to 16 for V-Ray and 24 for mental ray.

In spite of the Maxwell renderer's ease of use, its algorithms are physically the most realistic with a very long rendering time, which is in general 7 to 10 times higher compared to that of mental ray and V-Ray. Unfortunately, due to the small number of parameters that a user of Maxwell renderer can manipulate, this time can hardly be reduced. On the other hand, in mental ray and V-Ray the user has more possibilities to change the settings and their combinations and therefore to costumize the rendering procedure and to affect the result.

To ensure an unbiased comparison, renderings of the three engines were corrected with light setting correction within each engine and using identical gamma value (2.2). Despite a good visual match of final renderings after the correction, the obtained colour differences ($\Delta E^*_{ab}$) between outputs of different engines were on average higher than 7.0 (measured on 19 different regions of interest).
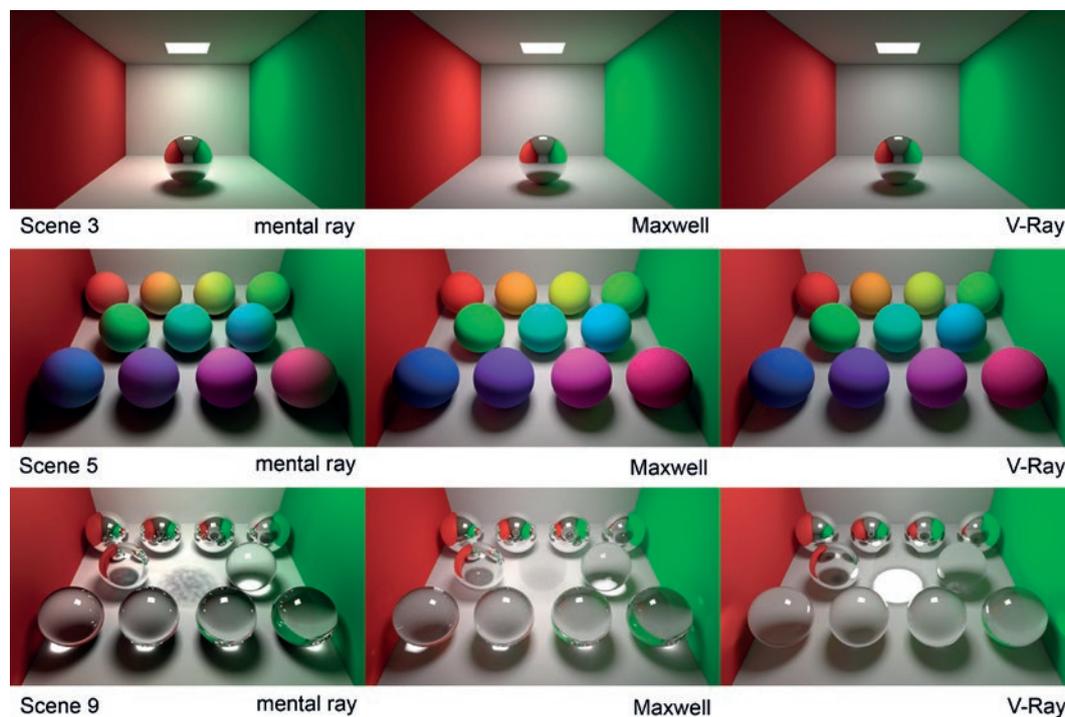


*Figure 6. Renderings of the scene no. 3 with a mirror material, the scene no. 5 with a colour diffuse material and scene no. 9 with different refraction indices of the spheres rendered with mental ray, Maxwell Render and V-Ray.*

19 regions of interest were also numerically evaluated for each rendering engine, resulting in a higher chrominance (chroma and hue) range between different regions of interest for Maxwell renderer and lower range of this colour feature for V-Ray. Mental ray rendering, on the other hand, resulted in higher brightness range between different areas of interests.

In the analysis of colourimetrical deviations between representative regions, Maxwell and mental ray renderer demonstrated better performance compared to V-Ray. Image pixels in mental ray rendering were in general reproduced with the highest differences in lightness (and also $\Delta E^*_{ab}$ values), while Maxwell renderer reproduced regions on red and green walls (red wall: ROIs 1 and 2; green wall: ROIs 4 and 5) and regions on the sphere (11, 12, 13 and 15) with higher chroma range (high $\Delta C^*_{ab}$ value between ROIs 11 and 15 and high $\Delta E^*_{ab}$ values between ROIs 12, 13 and 15).

When one wants to compare outputs of different engines, rendering parameters should be set separately for each material used. That was evident especially in the case of V-Ray engine and a transparent material where with the pre-defined rendering settings (defined on a diffuse material, scene 1) different reproductions of refraction and missing refraction of objects in the spheres were present.

When focusing on the renderer usability aspect, we can conclude that Maxwell renderer should be used when rendering time is less important, and we are primarily interested in an easy to use and simple user interface, with few rendering options. Mental ray was found to be the most complex engine, with many settings and their combinations, which, with the proper knowledge and understanding, can result in excellent renderings and low rendering time. Finally, the average user will spend less time to understand the settings of V-Ray, which proved to be less complex than mental ray, producing also excellent renderings. However, with an increased scene complexity rendering times for V-Ray increase faster than in the case of mental ray.

## References

Adamsen, M., 2009. Bidirectional Path Tracer (online). Available at: http://www.maw.dk/?page_id=78 (accessed: 10.1.2014).

Appel, A., 1968. Some techniques for shading machine renderings of solids. Proceedings of the Spring Joint Computer Conference 32, pp. 37–49.

Birn, J., 2013. Digital Lighting and Rendering, 3rd Ed. New Jersey: New Riders.

Bogolepov, D., Ulyanov, D., Sopin, D., Turlapov, V., 2013. GPU-Optimised Bi-Directional Path Tracing for modeling Optical Experiments. Scientific Visualization, Q. 2, Vol. 5, No. 2, pp. 1-15.

Bouknight W. J., 1970. A procedure for generation of three-dimensional half-toned computer graphics presentations. Communications of the ACM, Vol. 13 No. 9, pp. 527-536

Bui, T. P., 1975. Illumination for computer generated pictures. Communications of the ACM , Vol. 18 No. 6. pp. 311–316.

Blinn F. J., Newell E. M., 1976. Texture and reflection in computer generated images. Communications of the ACM, Vol 19 No. 10, pp. 542–547.

Csébfalvi, B., 1997. A Review of Monte-Carlo and Quasi-Monte Carlo Ray-Tracing Algorithms - Related Work (online) Available at: http://www.fsz.bme.hu/~szirmay/mcrt/node6.html (accessed 22. march 2014).

Erzetič, B., Gabrijelčič, H., 2010. 3D od točke do upodobitve. 2nd Ed.  Ljubljana : Pasadena.

Fleming, R.W., Dror, R.O., Adelson, E.H., 2003. Real-world illumination and the perception of surface reflectance properties. Journal of Vision, Vol. 3, No. 5, pp. 347-368.

Goesele, M., Lensch, H. P. A., Seidel, H. P., 2004. Validation of color managed 3D appearance aquisition, Society for Imaging Science and Technology, Proceeding of the Color and Imaging Conference, 12th Color and Imaging Conference Final Program and Proceedings, pp. 265-270 (6).

Goral, M. C., Torrance E. K., Greenberg, P.D., Battaile, B., 1984. Modeling the Interaction of Light Between Diffuse Surfaces. ACM SIGGRAPH Computer Graphics, Vol.18, No. 3, pp. 213-222.

Hunt, R. W. G. & Pointer M. R., 2011. Measuring Color, 4. Ed. Chichester, West Sussex: Wiley.

ImageJ, 2014. Image Processing and Analysis in Java (online). Available at: http://rsbweb.nih.gov/ij/ (accessed 14 February 2014).

Jensen, W. H., 2001. Realistic image synthesis using photon mapping, 2nd Ed. Massachusetts, Florida: A K Peters/CRC Press.

Jensen, W. H., 2002. A Practical Guide to Global Illumination using Photon Mapping (online). Available at: http://www.cs.princeton.edu/courses/archive/fall02/cs526/papers/course43sig02.pdf (accessed 22 March 2014).

Kajiya, J. T., 1986. The rendering equation. Proceedings of the 13th annual conference on Computer graphics and interactive techniques, pp. 143-150.

Kočevar, T. N., Gabrijelčič Tomc, H., 2013. Primerjava 3D simulacij tekstilij z oceno uporabe dveh aplikacij in slikovno analizo upodobitev = Comparison of 3D Textile Simulations with Evaluation of Usability of Two Applications and Image Analysis of Renderings. Tekstilec, Vol. 56, No. 4, pp. 323–334.

Kouhzadi, A., Rasti, A., Rasti, D., Why, N. K., 2013. Unbiased Monte Carlo Rendering – A Comparison Study.

International Journal of Scientific Knowledge. Vol. 2, No.3, pp. 1-10.

Krishnamachari, P., 2004. Global Illumination in a Nutshell (online). Available at: http://www.thepolygoners.com/tutorials/GIIntro/GIIntro.htm (accessed 22. march 2014).

Lafortune, E. P. & Willems, Y. D., 1993. Bi-directional Path Tracing. In Santo, H. P., editor, Proceedings of Third International Conference on Computational Graphics and Visualization Techniques (Compugraphics '93, Alvor, Portugal), pp. 145–153.

Luxrender, 2013. LuxRender Render settings (online). Available at: http://www.luxrender.net/wiki/LuxRender_Render_settings (accessed 20 march 2014).

Maxwell Render V3, 2014. Maxwell Render V2 Documentation - Next Limit Technologies (online). Available at: http://support.nextlimit.com/display/maxwelldocs/Maxwell+Render+V2+Documentation (accessed 23 March 2014).

Maxwell Render, 2014. Maxwell Render, Next Limit Technologies (online). Available at: http://www.maxwellrender.com (accessed 23 March 2014).

Menk, C., Koch, R., 2013. Truthful Color Reproduction in Spatial Augmented Reality Applications. IEEE Transactions on Visualization and Computer Graphics, Vol. 19, No. 2, pp. 236-248.

Murat, K., Dave, E., 2009. A survey of BRDF models for computer graphics, ACM SIGGRAPH Computer Graphics - Building Bridges - Science, the Arts & Technology, Vol. 43 No. 2.

O'Connor, J., 2010. Mastering mental ray: Rendering Techniques for 3D and CAD Professionals 1st. ed. Sybex.

Paviotti, A., Brusco, N., Cortelazzo G.M., 2007. Full automation and true colors in 3D modeling of cultural heritage. SPIE Newsroom. (online). Available at: http://spie.org/x14220.xml?pf=true (accessed 30. 1. 2014).

Pajot, A., Barthe, L., Paulin, M., Poulin P., 2011. Combinatorial Bidirectional Path Tracing For Efficient Hybrid CPU/GPU Rnedering. EuroGraphics 2001, Vol. 30, No. 2, pp. 316-324.

Pharr, M., Humphreys, G., 2010. Physically Based Rendering, Second Ed.: From Theory To Implementation, Burlington, Massachusetts: Morgan Kaufmann.

Ruppertsberg, A. I. & Bloj, M ., 2007. Reflecting on a room of one reflectance, Journal of Vision, Vol. 7 (13), No. 12, pp. 1-13.

Russ, C. J., 201. The Image Processing Handbook, 6th ed. Boca Raton, Florida : CRC Press.

Sannino, C. (2013) Photography & Rendering with V-Ray, Assemini (CA) : GC edizioni.

Xiao B., Brainard H.  D., 200. Surface gloss and color perception of 3D objects, Visual Neuroscience , Vol. 25 No.  03,  p. 371-385.

Yafaray, 2009. Lighting methods (online). Available at:  www.yafaray.org/documentation/userguide/lightingmethods (accessed 20 march 2014).

Whitted, T., 1980. An improved illumination model for shaded display. Communications of the ACM , Vol. 23, No. 6, pp. 343–349.